

Finite-temperature conductance signatures of quantum criticality in double quantum dots

Luis G. G. V. Dias da Silva,^{1,2} Kevin Ingersent,³ Nancy Sandler,¹ and Sergio E. Ulloa¹

¹*Department of Physics and Astronomy and Nanoscale and Quantum Phenomena Institute,*

Ohio University, Athens, Ohio 45701-2979, USA

²*Materials Science and Technology Division, Oak Ridge National Laboratory, Oak Ridge, Tennessee 37831, USA*
 and *Department of Physics and Astronomy, University of Tennessee, Knoxville, Tennessee 37996, USA*

³*Department of Physics, University of Florida, P.O. Box 118440, Gainesville, Florida, 32611-8440, USA*

(Received 13 September 2008; published 9 October 2008)

We study the linear conductance through a double-quantum-dot system consisting of an interacting dot in its Kondo regime and an effectively noninteracting dot connected in parallel to metallic leads. Signatures in the zero-bias conductance at temperatures $T > 0$ mark a pair of quantum ($T=0$) phase transitions between a Kondo-screened many-body ground state and non-Kondo ground states. Notably, the conductance features become more prominent with increasing T , which enhances the experimental prospects for accessing the quantum-critical region through tuning of gate voltages in a single device.

DOI: [10.1103/PhysRevB.78.153304](https://doi.org/10.1103/PhysRevB.78.153304)

PACS number(s): 73.63.Kv, 72.15.Qm

I. INTRODUCTION

Quantum phase transitions (QPTs) occur in the zero-temperature ($T=0$) phase diagram of a system at points of nonanalyticity of the ground-state energy.^{1,2} QPTs underlie many fascinating phenomena in strongly interacting condensed matter including the metal-insulator transition in disordered systems,³ the destruction of antiferromagnetism with doping in high-temperature superconductor parent compounds,⁴ the magnetic-field-driven superconducting-insulator transition in disordered superconductors,⁵ and quantum Hall plateau transitions.⁶ Study of most of these QPTs is hindered by the need to fabricate controlled series of samples at different stoichiometries and/or disorder levels.

By contrast, it is increasingly apparent that systems of quantum dots offer possibilities for exploring QPTs (strictly, *boundary* QPTs involving only a subset of the system degrees of freedom) within a single sample. Advances in system fabrication, precise characterization, and the near suppression of dissipative and incoherent environments⁷ have enabled beautiful experiments on multidot devices.⁸ This leap forward in experimental capability has also spurred much theoretical activity including several predictions of QPTs in quantum dots in the Kondo regime.⁹ The feasibility of realizing nontrivial many-body states has been confirmed by the recent experimental demonstrations of a two-channel Kondo regime¹⁰ and of a singlet-triplet QPT.¹¹

This Brief Report predicts robust signatures of QPTs in the finite-temperature conductance through a double-quantum-dot (DQD) system. A smaller dot (“dot 1”) exhibits Kondo physics, while a larger dot (“dot 2”) is effectively noninteracting and lies near a transmission resonance. When the dots are connected in parallel to external leads, and the system is fine tuned via applied voltages that determine tunneling barriers and the energies of individual dot orbitals, a *pseudogap* in the low-energy effective hybridization between dot 1 and the leads gives rise to a pair of continuous QPTs between Kondo-screened and non-Kondo ground states.¹² We describe how the system can be steered into the vicinity of a QPT by monitoring the linear conductance while changing just two gate voltages.

Experimental detection of QPTs necessarily relies on finite-temperature manifestations of the underlying $T=0$ transition. We show that the signatures of quantum criticality in the present DQD system become more pronounced as the temperature is increased from absolute zero—a trend that contrasts with the typical behavior near an impurity QPT.² Their temperature dependence also allows these signatures to be distinguished from other conductance features in the same system.

II. MODEL AND CONDUCTANCE CALCULATION

Consider a DQD device in which dot 1 is in an odd-electron-number Coulomb blockade valley and dot 2 has a single level near the Fermi level and is effectively noninteracting.¹³ The dots are coupled to left (L) and right (R) metallic leads and to each other via tunneling barriers. This device is described by a two-impurity Anderson Hamiltonian,

$$H = \sum_{i,\sigma} \varepsilon_i n_{i\sigma} + U_1 n_{1\uparrow} n_{1\downarrow} + \sum_{\sigma} (\lambda a_{1\sigma}^\dagger a_{2\sigma} + \text{H.c.}) + \sum_{\ell,\mathbf{k},\sigma} \varepsilon_{\ell\mathbf{k}} c_{\ell\mathbf{k}\sigma}^\dagger c_{\ell\mathbf{k}\sigma} + \sum_{i,\ell,\mathbf{k},\sigma} (V_{i\ell} a_{i\sigma}^\dagger c_{\ell\mathbf{k}\sigma} + \text{H.c.}), \quad (1)$$

where $a_{i\sigma}^\dagger$ creates a spin- σ electron in dot i ($i=1,2$), $n_{i\sigma} = a_{i\sigma}^\dagger a_{i\sigma}$, and $c_{\ell\mathbf{k}\sigma}^\dagger$ creates a spin- σ electron of wave vector \mathbf{k} and energy $\varepsilon_{\ell\mathbf{k}}$ in lead ℓ ($\ell=L,R$). We assume for simplicity that each lead has a density of states, $\rho(\omega) = \rho_0 \Theta(D - |\omega|)$, symmetric about the Fermi energy ($\omega=0$) and that dot-lead couplings are local. We further assume that all couplings are real and the device is tuned to left-right symmetry so that we can write $V_{i\ell} = V_i / \sqrt{2}$.

The linear conductance at temperature T for this DQD setup can be obtained from the Landauer formula as

$$g(T) = g_0 \int_{-\infty}^{\infty} d\omega (-\partial f / \partial \omega) [-\text{Im } \mathcal{T}(\omega)], \quad (2)$$

$$\mathcal{T}(\omega) = 2\pi\rho_0 \sum_{i,j} V_{iL}^* G_{ij}(\omega) V_{jR}, \quad (3)$$

where $g_0 = 2e^2/h$, $f(\omega/T) = [\exp(\omega/T) + 1]^{-1}$ is the Fermi-Dirac function, and all $G_{ij}(\omega)$ in Eq. (3) are dressed Green's functions, fully taking into account the electron-electron interactions on dot 1.

The standard equations of motion $\omega \langle\langle A; B \rangle\rangle_\omega - \langle\{A, B\}\rangle = \langle\langle [A, H]; B \rangle\rangle_\omega = -\langle\langle A; [B, H] \rangle\rangle_\omega$ for the retarded Green's function $\langle\langle A; B \rangle\rangle_\omega = -i \int_0^\infty dt e^{i\omega t} \langle\{A(t), B(0)\}\rangle$ allow one to re-express $G_{ij}(\omega) = \langle\langle a_{i\sigma}; a_{j\sigma}^\dagger \rangle\rangle_\omega$ in terms of G_{11} and the bare Green's function $G_{22}^{(0)}$, which describes the noninteracting dot 2 in the absence of dot 1. In the wide-band limit $|\omega| \ll D$,¹³ Eq. (3) becomes

$$\mathcal{T}(\omega) = \Delta_1 G_{11}(\omega) + 2\Delta_{12} [G_{22}^{(0)}(\omega)(\lambda - i\Delta_{12})G_{11}(\omega)] + \Delta_2 [1 + G_{22}^{(0)}(\omega)(\lambda - i\Delta_{12})^2 G_{11}(\omega)] G_{22}^{(0)}(\omega), \quad (4)$$

where $\Delta_i = \pi\rho_0 V_i^2$, $\Delta_{12} = \pi\rho_0 V_1 V_2$, and $G_{22}^{(0)}(\omega) = (\omega - \varepsilon_2 + i\Delta_2)^{-1}$.

The dot-1 local Green's function $G_{11}(\omega)$ entering Eq. (4) can be obtained¹² by mapping the Hamiltonian (1) to an effective model of a single dot connected to the leads via a nonconstant hybridization function,

$$\Delta(\omega) = \pi\rho_2(\omega) [\lambda + (\omega - \varepsilon_2) \sqrt{\Delta_1/\Delta_2}]^2, \quad (5)$$

with $\rho_2(\omega) = \Delta_2 / \{\pi[(\omega - \varepsilon_2)^2 + \Delta_2^2]\}$. We solve this effective model using the numerical renormalization group.¹⁴ At $T > 0$, we compute the spectral function $A_{11}(\omega) = -\pi^{-1} \text{Im} G_{11}(\omega)$, and hence, we obtain $G'_{11}(\omega) = \text{Re} G_{11}(\omega)$ via a Kramers-Kronig transformation. At $T = 0$, where Eq. (2) involves only $G_{11}(0)$, it is possible to calculate $G'_{11}(0)$ directly. All results shown are for $U_1 = 0.5D$ and $\Delta_2 = 0.02D$ with temperatures in units of $T_{K0} = 7.0 \times 10^{-4}D$ [the Kondo temperature in the reference case where dot 2 is decoupled ($\lambda = \Delta_2 = 0$) and $U_1 = -2\varepsilon_1 = 0.5D$ and $\Delta_1 = 0.05D$].

To facilitate interpretation of the results, we note that $-\text{Im} \mathcal{T}(\omega)$ entering Eq. (2) can be expressed as

$$-\text{Im} \mathcal{T}(\omega) = [1 - 2\pi\Delta_2\rho_2(\omega)]\pi\Delta(\omega)A_{11}(\omega) + \pi\Delta_2\rho_2(\omega) + 2\pi(\omega - \varepsilon_2)\Delta(\omega)\rho_2(\omega)G'_{11}(\omega). \quad (6)$$

The term $\pi\Delta_2\rho_2(\omega)$ represents bare transmission through dot 2 in the absence of dot 1, and for $T \ll \Delta_2$ it yields a conductance contribution $g_2 \approx g_0 \Delta_2^2 / (\varepsilon_2^2 + \Delta_2^2)$. In most cases of interest, the term involving G'_{11} turns out to be negligible. If, as we assume, the dot-1 level is off resonance (i.e., $|\varepsilon_1| \gg T, \Delta_1$), then dot 1 appreciably influences g only in the Kondo regime $T \lesssim T_K$ where $A_{11}(\omega)$ exhibits a many-body resonance at the Fermi level; the sign of the resulting conductance term g_1 depends on that of $1 - 2\pi\Delta_2\rho_2(\omega)$ in the range $|\omega| \lesssim O(T)$ that determines $g(T)$. For $|\varepsilon_2| \gg \Delta_2$ ($|\varepsilon_2| \ll \Delta_2$), g_1 is positive (negative) at low temperatures, leading to constructive (destructive) interference with g_2 .

III. TUNING TO THE PSEUDOGAP REGIME

When the level energy in dot 2 is set to $\varepsilon_2 = \lambda \sqrt{\Delta_2/\Delta_1}$, the dot-1 effective hybridization [Eq. (5)] vanishes at the Fermi

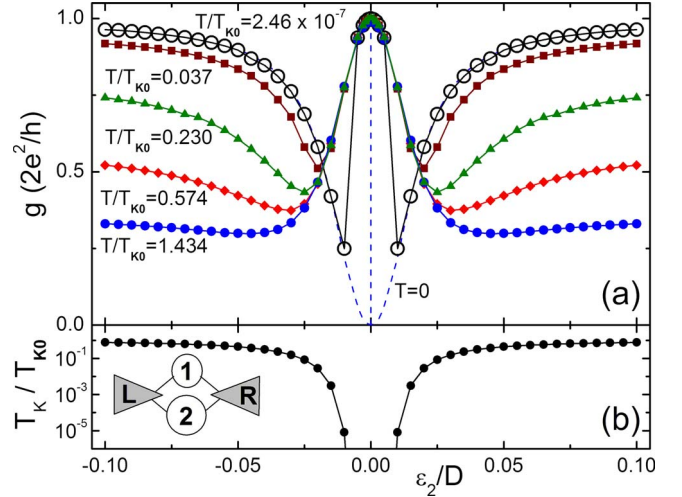


FIG. 1. (Color online) (a) Conductance g vs ε_2 at six temperatures for a *parallel* DQD device [inset of (b)] with $\varepsilon_1 = -U_1/2$ and $\Delta_1 = 0.05D$. (b) Transmission through dot 1 sets in below the Kondo temperature T_K (defined as in Ref. 12), which vanishes as $\varepsilon_2 \rightarrow 0$.

level as $\Delta(\omega) \propto \omega^2$. The pseudogap Anderson impurity model, in which $\Delta(\omega) \propto |\omega|^r$ for $|\omega| \rightarrow 0$, exhibits Kondo and non-Kondo ground states separated by QPTs. Whereas previous theoretical work¹⁵ has focused on exponents $0 < r \leq 1$, the proposed DQD setup offers a controlled realization of the case $r=2$, which features a pair of QPTs. For simplicity, we focus in the remainder of this Brief Report on configurations in which the dots are connected to the leads purely in parallel, i.e., $\lambda=0$ [see inset of Fig. 1(b)]. Then Eq. (5) reduces to $\Delta(\omega) = \Delta_1(\omega - \varepsilon_2)^2 / [(\omega - \varepsilon_2)^2 + \Delta_2^2]$.

In order to probe the QPTs, the pseudogap in $\Delta(\omega)$ must be centered on the Fermi energy. Operationally, this can be accomplished by tuning ε_2 (via a plunger gate voltage on dot 2) to reach a maximum of g . Figure 1(a) illustrates g vs ε_2 at six temperatures for fixed $\varepsilon_1 = -U_1/2$ and $\Delta_1 = 0.05D$. For $\lambda = 0$, $\Delta(0) = 0$ when dot 2 is exactly in resonance with the leads: $\varepsilon_2 = 0$. The choice of $\varepsilon_1 = -U_1/2$ makes $\varepsilon_2 = 0$ a point of particle-hole (p - h) symmetry and ensures that for $|\varepsilon_2| \ll \Delta_2$ and $T \ll T_K$, $\pi\Delta(0)A_{11}(0) \approx 1$;¹⁶ then, since $\pi\Delta_2\rho_2(0) \approx 1$, g_1 almost completely cancels g_2 . Figure 1(b) shows that the temperature range $0 \leq T \leq T_K(\varepsilon_2)$ of the low-conductance regime shrinks rapidly as $\varepsilon_2 \rightarrow 0$. For the special case $\varepsilon_2 = 0$, the pseudogap in $\Delta(\omega)$ prevents the formation of a Kondo state (effectively, $T_K = 0$), and transport takes place solely through dot 2. At $T = 0$, the resulting conductance exhibits a discrete jump from $g = 0$ for $|\varepsilon_2| \rightarrow 0$ to $g = g_0$ for $\varepsilon_2 = 0$ [dashed line in Fig. 1(a)]. However, this spike broadens at $T > 0$ into a smooth peak rising to $g(\varepsilon_2 = 0) \approx g_0$.

For a general $\varepsilon_1 \neq -U_1/2$, transmission through dot 1 is still blocked when $\Delta(0) = 0$. This leads to an asymmetric peak in $g(\varepsilon_2)$ at $g(0) \approx g_0$ —a feature that again broadens with increasing T ,¹⁷ offering a practical method for tuning the pseudogap to the Fermi level.

IV. TUNING TO A QPT

With ε_2 held at zero, the level energy ε_1 can be varied via a plunger gate voltage on dot 1. A pair of QPTs, related by

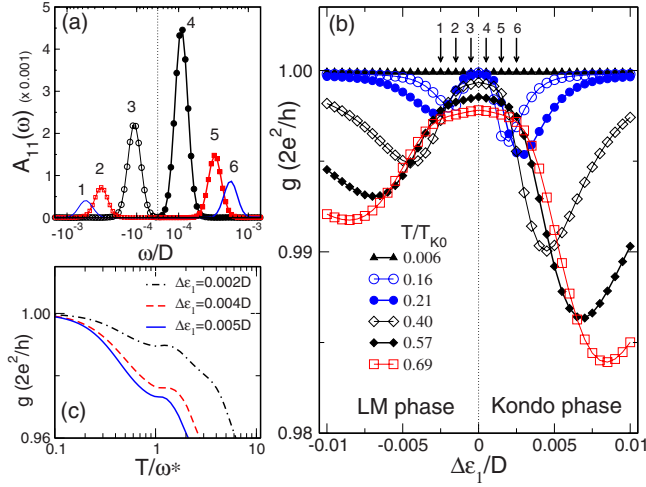


FIG. 2. (Color online) Behavior near the ε_{1c}^+ transition in a parallel DQD device with $\Delta_1=0.05D$ and $\varepsilon_2=0$. (a) Curves 1–6 show the dot-1 spectral function $A_{11}(\omega)$ for the values of $\Delta\varepsilon_1=\varepsilon_1-\varepsilon_{1c}^+$ indicated by the corresponding arrows in (b). The frequency ω^* of the quasiparticle peak in $A_{11}(\omega)$ is proportional to $\Delta\varepsilon_1$. (b) Conductance g vs $\Delta\varepsilon_1$ at six temperatures. (c) g vs T/ω^* at three values of $\Delta\varepsilon_1$ on the Kondo side of the transition.

p - h duality and located at $\varepsilon_1=\varepsilon_{1c}^\pm=-U_1/2\pm|\Delta\varepsilon_{1c}|$, bound a local-moment (LM) regime $\varepsilon_1^-<\varepsilon_1<\varepsilon_{1c}^+$ in which the net spin on dot 1 is unscreened at $T=0$. Close to either QPT, $A_{11}(\omega)$ contains a quasiparticle peak centered at $\omega=\omega^*$, where $\omega^*\propto\varepsilon_1-\varepsilon_{1c}^\pm$ [Fig. 2(a)]. The peak sets in below a crossover temperature $\approx|\omega^*|$, which on the Kondo side is proportional to T_K . This feature in $A_{11}(\omega)$ leads, via Eqs. (2) and (6), to a conductance contribution $g_1<0$ that is greatest in magnitude when $|\omega^*|\approx 4T$. Since the dot-2 contribution $g_2\approx g_0$ is independent of ε_1 , g vs ε_1 isotherms [e.g., see Fig. 2(b)] show a dip at $|\varepsilon_1-\varepsilon_{1c}^\pm|\propto T$ on either side of a maximum at $\varepsilon_1=\varepsilon_{1c}^\pm$.

It is striking that at $T=0$, the conductance shows no feature as dot 1 passes through a QPT. At finite temperatures, by contrast, the DQD device can be tuned to the transition by seeking a local maximum in g vs ε_1 . This maximum has the identifying characteristics [Fig. 2(b)] that the minima on either side are equidistant in ε_1 from ε_{1c}^\pm , but the dip in g is roughly twice as deep on the Kondo side, reflecting the greater weight of the quasiparticle peak in that regime. For the parameters shown in Fig. 2(b), the conductance peak becomes more prominent with increasing temperature up to $T\approx 3T_{K0}$, and a peak in g remains discernible up to the relatively high scale $T\approx 6T_{K0}$.

The form of g vs T at fixed ε_1 is more complicated since g_1 and g_2 can have temperature variations of comparable magnitude. Figure 2(c) shows that in the Kondo regime, the peak in $|g_1(T)|$ contributes a shoulder around $T=|\omega^*|$ to the overall downward trend dictated by $g_2(T)$. Similar behavior holds in the LM regime (not shown).

V. UNIQUENESS OF QPT SIGNATURES

Conductance peaks similar to those shown in Fig. 2(b) can also arise not from proximity to a QPT but rather from

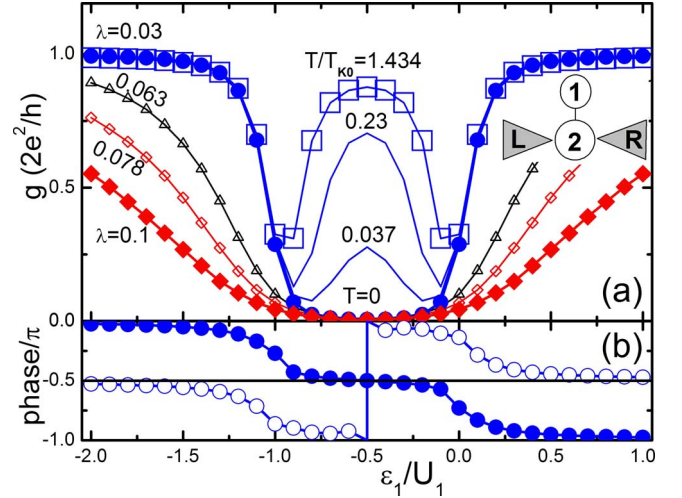


FIG. 3. (Color online) (a) Conductance g vs ε_1 for a side-dot device (inset) with $\varepsilon_2=0$ both for $T=0$ at various λ values and for $\lambda=0.03D$ at the labeled temperatures. (b) Phase shifts η_{11} (filled circles) and η_{22} (open circles) for $\lambda=0.03D$ and $T=0$; g vanishes when $\sin\eta_{22}=0$ [Eq. (7)].

interference between a conventional (metallic or $r=0$) many-body Kondo resonance on dot 1 and a noninteracting resonance on dot 2. In experiments, the mapping between the gate voltages in a real device and parameters of the effective Anderson model will not be known *a priori*. It is therefore important to be able to identify unique signatures of a QPT in this system. We show below that the temperature dependence of the conductance peaks serves this purpose.

For simplicity, we consider the “side-dot” regime¹⁸ $\Delta_1=0$ in which dot 1 is connected to the leads only via the noninteracting dot 2. In this geometry [inset of Fig. 3(a)], the effective dot-1 hybridization function $\Delta(\omega)=\pi\lambda^2\rho_2(\omega)$ [from Eq. (5)] is a Lorentzian of width Δ_2 centered at $\omega=\varepsilon_2$. Since $\Delta(\omega)$ has no pseudogap, there is no QPT.

Figure 3 plots the variation of the conductance with the position ε_1 of the energy level in the side dot 1 while dot 2 is held in resonance, i.e., $\varepsilon_2=0$. At $T=0$, and for all values of the dot-dot coupling λ , the conductance drops to zero as ε_1 approaches the p - h -symmetric point $\varepsilon_1=-U_1/2$. This can be understood by noting that for $\Delta_1=0$ and $T=0$, Eqs. (2) and (3) reduce to

$$g(T=0)=-g_0\Delta_2|G_{22}(0)|\sin\eta_{22}, \quad (7)$$

where $\eta_{ii}=\arg G_{ii}(0)$ is the Fermi-energy phase shift of electrons scattering from dot i . Figure 3(b) shows that in a window about the p - h -symmetric point, the dot-1 phase shift exhibits a plateau $\eta_{11}\approx-\pi/2$ characteristic of the Kondo state.¹⁹ This additional phase shift of electrons that scatter from the side dot on their path between the two leads renormalizes the bare dot-2 phase shift $\eta_{22}^{(0)}=-\pi/2$ to produce an η_{22} that jumps from $-\pi$ to 0 at the p - h point. On moving away from $\varepsilon_1=-U_1/2$, dot 1 gradually enters its mixed-valence regime, where there is no Kondo resonance and the $T=0$ conductance rises toward its unitary limit $g=g_0$. With increasing λ , the Kondo state in dot 1 becomes more robust

(as evidenced¹² by its larger T_K), pushing this upturn in g to larger values of $|\varepsilon_1 + U_1/2|$.

Raising the temperature progressively destroys the Kondo resonance and thereby increases the conductance. For fixed $T > 0$, g vs ε_1 reaches a peak at $\varepsilon_1 = -U_1/2$, where T_K is smallest and Kondo scattering is weakest. Figure 3(a) illustrates this behavior at three temperatures for $\varepsilon_2 = 0$ and $\lambda = 0.03D$. The double-dip structure surrounding the peak in g vs ε_1 is qualitatively similar to the QPT feature in Fig. 2(b). However, the temperature variation is very different in the two cases. In Fig. 2(b), the *decrease* with increasing T of the conductance both at the peak and at the minima on either side is a characteristic of the QPT. By contrast, conductance peaks arising for $\Delta(0) \neq 0$ exhibit an *increase* with T of the extremal g values as seen in Fig. 3(a).

VI. CONCLUSION

To conclude, we have studied the linear conductance through a class of quantum-dot devices that can be described

by a single Anderson impurity coupled to a conduction band via a nonconstant hybridization function. Such devices can be tuned to a quantum phase transition marked by a near-unitary peak in the linear conductance that becomes more pronounced with increasing temperatures. The details of its evolution with temperature differentiate this conductance signature from similar features arising from interference effects unrelated to quantum criticality. Our results demonstrate that these quantum-dot devices offer many advantages for the controlled experimental investigation of a rich array of many-body physics.

ACKNOWLEDGMENTS

We thank C. Lewenkopf, C. Büsser, and E. Vernek for valuable discussions, and we acknowledge support from NSF-DMR under Grants No. 0312939, No. 0710540 (Florida), No. 0336431, No. 0304314, No. 0710581 (Ohio), and No. 0706020 (Tennessee).

¹S. Sachdev, *Quantum Phase Transitions* (Cambridge University Press, Cambridge, UK, 1999).

²M. Vojta, *Philos. Mag.* **86**, 1807 (2006).

³A. Husmann, X. Yao, D. S. Jin, Y. V. Zastavker, T. F. Rosenbaum, and J. M. Honig, *Science* **274**, 1874 (1996).

⁴S. Sachdev, *Rev. Mod. Phys.* **75**, 913 (2003).

⁵N. Mason and A. Kapitulnik, *Phys. Rev. Lett.* **82**, 5341 (1999).

⁶S. L. Sondhi, S. M. Girvin, J. P. Carini, and D. Shahar, *Rev. Mod. Phys.* **69**, 315 (1997).

⁷D. Goldhaber-Gordon, H. Shtrikman, D. Mahalu, D. Abusch-Magder, U. Meirav, and M. S. Kastner, *Nature (London)* **391**, 156 (1998).

⁸H. Jeong, A. M. Chang, and M. R. Melloch, *Science* **293**, 2221 (2001); N. J. Craig, J. M. Taylor, E. A. Lester, C. M. Marcus, M. P. Hanson, and A. C. Gossard, *ibid.* **304**, 565 (2004); J. C. Chen, A. M. Chang, and M. R. Melloch, *Phys. Rev. Lett.* **92**, 176801 (2004); A. Fuhrer, T. Ihn, K. Ensslin, W. Wegscheider, and M. Bichler, *ibid.* **93**, 176803 (2004); R. Leturcq, L. Schmid, K. Ensslin, Y. Meir, D. C. Driscoll, and A. C. Gossard, *ibid.* **95**, 126603 (2005).

⁹W. Hofstetter and H. Schoeller, *Phys. Rev. Lett.* **88**, 016803 (2001); M. Pustilnik, L. Borda, L. I. Glazman, and J. von Delft, *Phys. Rev. B* **69**, 115316 (2004); M. R. Galpin, D. E. Logan, and H. R. Krishnamurthy, *Phys. Rev. Lett.* **94**, 186406 (2005); G. Zarand, C. H. Chung, P. Simon, and M. Vojta, *ibid.* **97**, 166802 (2006); R. Zitko and J. Bonca, *Phys. Rev. B* **76**, 241305(R) (2007).

¹⁰R. M. Potok, I. G. Rau, H. Shtrikman, Y. Oreg, and D. Goldhaber-Gordon, *Nature (London)* **446**, 167 (2007).

¹¹N. Roch, S. Florens, V. Bouchiat, W. Wernsdorfer, and F. Balestro, *Nature (London)* **453**, 633 (2008).

¹²L. G. G. V. Dias da Silva, N. P. Sandler, K. Ingersent, and S. E. Ulloa, *Phys. Rev. Lett.* **97**, 096603 (2006); **99**, 209702 (2007).

¹³The assumptions of a noninteracting dot 2 and a wide band simplify the analysis, but essentially the same properties arise from the full solution of Eq. (1) for a weakly interacting dot 2, as will be discussed elsewhere (Ref. 17).

¹⁴R. Bulla, T. A. Costi, and T. Pruschke, *Rev. Mod. Phys.* **80**, 395 (2008).

¹⁵D. Withoff and E. Fradkin, *Phys. Rev. Lett.* **64**, 1835 (1990); C. Gonzalez-Buxton and K. Ingersent, *Phys. Rev. B* **54**, R15614 (1996); **57**, 14254 (1998); R. Bulla, Th. Pruschke, and A. C. Hewson, *J. Phys.: Condens. Matter* **9**, 10463 (1997); M. Vojta and R. Bulla, *Phys. Rev. B* **65**, 014511 (2001); L. Fritz and M. Vojta, *ibid.* **70**, 214427 (2004).

¹⁶L. Vaugier, A. A. Aligia, and A. M. Lobos, *Phys. Rev. Lett.* **99**, 209701 (2007).

¹⁷W. B. Lane, K. Ingersent, L. G. G. V. Dias da Silva, N. P. Sandler, and S. E. Ulloa (unpublished).

¹⁸K. Kang, S. Y. Cho, J.-J. Kim, and S. C. Shin, *Phys. Rev. B* **63**, 113304 (2001); V. M. Apel, M. A. Davidovich, E. V. Anda, C. A. Busser, and G. Chiappe, *Microelectron. J.* **34**, 729 (2003); C. A. Büsser, G. B. Martins, K. A. Al-Hassanieh, A. Moreo, and E. Dagotto, *Phys. Rev. B* **70**, 245303 (2004); P. S. Cornaglia and D. R. Grempel, *ibid.* **71**, 075305 (2005); P. Simon, J. Salomez, and D. Feinberg, *ibid.* **73**, 205325 (2006); R. Zitko and J. Bonca, *ibid.* **73**, 035332 (2006); P. A. Orellana, G. A. Lara, and E. V. Anda, *ibid.* **74**, 193315 (2006); A. C. Seridonio, M. Yoshida, and L. N. Oliveira, arXiv:cond-mat/0701529 (unpublished).

¹⁹U. Gerland, J. von Delft, T. A. Costi, and Y. Oreg, *Phys. Rev. Lett.* **84**, 3710 (2000).